Ag nanoparticle–ZnO nanowire hybrid nanostructures as enhanced and robust antimicrobial textiles via a green chemical approach

2014 Nanotechnology 25 145702

(http://iopscience.iop.org/0957-4484/25/14/145702)

IOP Publishing Nanotechnology
Nanotechnology **25** (2014) 145702 (8pp) doi:10.1088/0957-4484/25/14/145702

Ag nanoparticle–ZnO nanowire hybrid nanostructures as enhanced and robust antimicrobial textiles via a green chemical approach

Zhou Li[1,5], Haoying Tang[2,5], Weiwei Yuan[1,4,5], Wei Song[1], Yongshan Niu[1], Ling Yan[1], Min Yu[1], Ming Dai[1], Siyu Feng[1], Menghang Wang[1], Tengjiao Liu[2], Peng Jiang[2], Yubo Fan[1] and Zhong Lin Wang[3,4]

[1] Key Laboratory for Biomechanics and Mechanobiology of Ministry of Education, School of Biological Science and Medical Engineering, Beihang University, Beijing 100191, People's Republic of China
[2] National Center of Nanoscience and Technology, Beijing 100191, People's Republic of China
[3] School of Materials Science and Engineering, Georgia Institute of Technology, Atlanta, GA 30332, USA
[4] Beijing Institute of Nanoenergy and Nanosystems, Chinese Academy of Science, Beijing 100083, People's Republic of China

E-mail: yubofan@buaa.edu.cn and zhong.wang@mse.gatech.edu

Received 4 December 2013, revised 16 January 2014
Accepted for publication 4 February 2014
Published 12 March 2014

Abstract

A new approach for fabrication of a long-term and recoverable antimicrobial nanostructure/textile hybrid without increasing the antimicrobial resistance is demonstrated. Using *in situ* synthesized Ag nanoparticles (NPs) anchored on ZnO nanowires (NWs) grown on textiles by a 'dip-in and light-irradiation' green chemical method, we obtained ZnONW@AgNP nanocomposites with small-size and uniform Ag NPs, which have shown superior performance for antibacterial applications. These new Ag/ZnO/textile antimicrobial composites can be used for wound dressings and medical textiles for topical and prophylactic antibacterial treatments, point-of-use water treatment to improve the cleanliness of water and antimicrobial air filters to prevent bioaerosols accumulating in ventilation, heating, and air-conditioning systems.

Keywords: silver nanoparticles, ZnO nanowires, antibacterial activity, biocompatibility, antibacterial textiles

S Online supplementary data available from stacks.iop.org/Nano/25/145702/mmedia

(Some figures may appear in colour only in the online journal)

1. Introduction

Since the discovery of penicillin, antibiotics have saved countless lives and alleviated immeasurable suffering [1]. However, the overuse of antibiotics could result in a decreased human resistance to diseases by immune suppression and an increased antimicrobial resistance of bacteria [2, 3]. Most recently, global concern over the overuse of antibiotics has increased dramatically due to the appearance of a new bacterium named superbug NDM-1, which has an unprecedented level of resistance to nearly all antibiotics known today [4, 5]. The World Health Day in 2011 was devoted to antimicrobial resistance under the theme of 'No action today, no cure tomorrow',

[5] These authors contributed equally to this work.

which called for global policy response to control the spread of antimicrobial resistance [6].

As an alternative to antibiotics, the renaissance of utilizing silver as a broad-spectrum and highly active antimicrobial is an alternative choice [7]. Although the specific mechanism for the antimicrobial activity of silver nanoparticles (Ag NPs) is not fully understood, it is believed that nano-sized particles offer enhanced Ag^+ ion release and higher specific surface area than their bulk counterpart [8, 9]. Possible antimicrobial mechanisms as caused by Ag NPs are likely collapse of the bacterial membrane, inhibition of the function of sulfur-containing proteins and phosphorus-containing DNA, and deterioration of the respiratory chain in bacterial mitochondria [7, 9–15].

However, there are several major challenges that remain for employing Ag NPs as antimicrobial materials. First, it is desired that the size of Ag NPs is small enough (<10 nm), which will guarantee better antimicrobial efficiency compared with their bulk counterpart by virtue of high specific surface area and enhanced metal-ion release [8, 9, 16]. Additionally, long-term antimicrobial activity of Ag NPs requires both the absence of particle aggregation during storage and long-term bacterial suppression during use as well as suppressed surface oxidation [17]. Moreover, recoverable and reusable antimicrobial materials are of great importance for reducing silver exposure to avoid potential biological risk, including environmental, cytotoxicity and human health effects [16, 18]. Finally, green synthesis of Ag NPs without external toxic and corrosive reducing agents, organic solvents and stabilizer is another environmentally benign process to avoid potential biological risk for practical applications [17, 19, 20]. Tremendous effects have been devoted to possibly address these four major challenges. Liu *et al* have reported recoverable small-sized Ag NPs by mixing graphene oxide and oleylamine-capped Ag nanoparticles synthesized by reducing $AgNO_3$ in toluene [16]. Lv and co-workers reported long-term antimicrobial effect of Ag NPs on silicon nanowires (SiNWs) by reducing silver ions to form SiNW@AgNP nanostructures in the presence of NaOH [17].

In this paper, we demonstrate a new approach to address the four major challenges stated above. By anchoring *in situ* synthesized Ag NPs on ZnO nanowires (NWs) grown on textiles by a 'dip-in and light-irradiation' green chemical method, we obtained small-sized Ag NPs with relative uniform diameters. ZnO NWs can prevent the aggregation of Ag NPs, which ensures the long-term antimicrobial activity of the composites. The composites can be recovered and reused by simple uptake of the textiles to reduce silver exposure. Moreover, ZnO nanomaterial is biodegradable and biocompatible [21], exhibits the most diverse and abundant family of nanostructures [22–24] and has been designed for piezoelectric nanogenerators [25, 26], Schottky contacted biosensors [27], DNA delivery [28, 29], cancer-targeted optical imaging [30] and a series of novel nano/microdevices in the bio-interface [31–35]. ZnO is also an antimicrobial material, which can provide extra antimicrobial ability to Ag NPs by a synergistic effect [29, 36–39]. Thus, the use of ZnO NWs will not cause additional biological risk, while promoting the antimicrobial effect of Ag NPs. The Ag/ZnO/textile antimicrobial composites can be used for point-of-use water treatment for sterilization, wound dressings and medical textiles for topical and prophylactic antibacterial treatments, and antimicrobial air filters to prevent bioaerosols accumulating in ventilation, heating and air-conditioning systems.

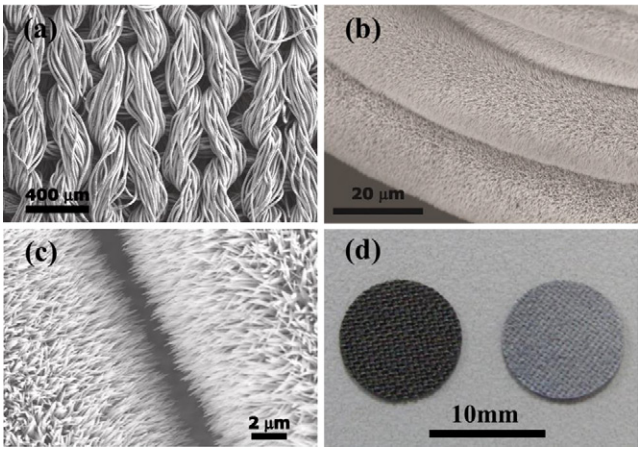

Figure 1. SEM and optical images of ZnO NWs grown on polyester textiles. (a) The overall view shows the insulating textiles can be imaged under electron irradiation due to the reduced charging effect on ZnO NW coverage. (b), (c) Magnified images show the ZnO NWs were grown on each textile fiber uniformly, with growth direction pointing outward, about 2 μm in length and 50–200 nm in diameter. (d) Before (left) and after (right) the growth of Ag NPs/ZnO NWs on polyester textile disks.

2. Results and discussion

ZnO NWs were grown on textiles by a two-step low-temperature seeded wet-chemical method [40]. Figure 1(a) shows the overall view of a scanning electron microscopy (SEM) image of the polyester textiles after growth. The insulating textiles can be imaged under electron irradiation due to the reduced charging effect on ZnO NW coverage. Figures 1(b), (c) show the magnified SEM images of the ZnO/textile hybrid. The ZnO NWs were grown on each textile fiber conformably, with the growth direction pointing outward. The lengths of the as-grown NWs were about 2 μm, with diameters in the range from 50 to 200 nm.

Silver NPs were loaded on the ZnO NWs by a simple 'dip-in and light-irradiation' green chemical method. ZnO/textile composites were first dipped in an ethanol–water solution of $AgNO_3$ for 24 h and then rinsed with ethanol for 30 s to remove unanchored ions. The Ag20/ZnO/textile (Ag20) composites were dipped in 20 mM $AgNO_3$ ethanol–water solution and Ag100/ZnO/textile (Ag100) composites were dipped in 100 mM $AgNO_3$ ethanol–water solution, respectively. The composites were then exposed under UV irradiation or left under natural light to reduce residual Ag ions to Ag NPs *in situ* on ZnO NWs. The UV–vis reflectance spectroscopy (figure 2(a)) of the Ag20/ZnO/textile composites shows two broad peaks centered at 370 and 435 nm, which correspond to the absorption edge of ZnO and characteristic surface plasmon peak of spherical Ag NPs, respectively [41]. Figure 2(b) shows a representative transmission electron microscopy (TEM) image

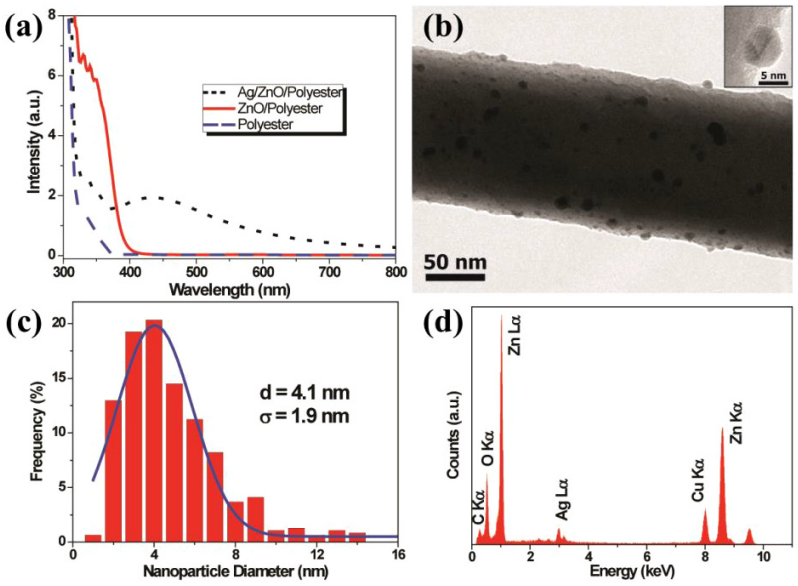

Figure 2. (a) UV–vis reflectance spectroscopy of the Ag/ZnO/textile composites shows two broad peaks centered at 370 nm and 435 nm, corresponding to the absorption edge of ZnO and the characteristic surface plasmon peak of spherical Ag nanoparticles, respectively. (b) TEM image of Ag/ZnO nanocomposites, showing that the Ag NPs were completely attached to ZnO NW without any aggregation. (c) Size distribution of Ag NPs. (d) The EDX spectrum confirms the formation of Ag in the samples.

of Ag20/ZnO nanocomposites (ZnONWs@AgNPs), showing that the Ag NPs were completely attached to ZnO NWs without aggregation. Ag NPs were grown relatively uniformly on ZnO nanowires with an average diameter of 4.1 nm and a standard deviation of 1.9 nm (figure 2(c)). Energy-dispersive x-ray spectroscopy (EDX) further confirms the formation of Ag in the samples, as indicated by the peak at around 3 keV in figure 2(d). The atomic ratio of Ag with respect to Zn was estimated to be from 1:10 to 1:20 in different samples by EDX in Ag20. Ag100 contains more silvers than Ag20. (See table S1 in the supporting information available at stacks.iop.org/Nano/25/145702/mmedia).

The formation of small Ag NPs on ZnO NWs is suggested to be a photochemical process [41, 42]. When the composites are subjected to UV light irradiation, photogenerated conduction band electrons (e^-_{CB}) and valence band holes (h^+_{VB}) will be created in ZnO NWs. The silver ions absorbed on the surface of ZnO during the 'dip-in' process will be reduced by the electrons trapped on the ZnO surface ($e^-_{trapped}$). Owing to the finite ion supply and multiple reaction centers on the surfaces, only small-size nanoparticles can be deposited on ZnO, and the large-size ones will be dropped out. This provides an excellent approach for selecting the small-size Ag NPs for our applications. The multiple reaction centers on the ZnO surface are surface defects emerging during the 'dip-in' process due to partially dissolved surface atoms of ZnO. The reaction process can be summarized as follows [41, 42]:

$$ZnO + h\nu \rightarrow ZnO(e^-_{CB} + h^+_{VB}) \quad (1)$$

$$e^-_{CB} \rightarrow e^-_{trapped} \quad (2)$$

$$Ag^+ + e^-_{trapped} \rightarrow Ag \quad (3)$$

where $h\nu$ is the light quantum.

ZnO NWs and Ag NPs for biological applications have been widely documented, respectively [26, 27, 36], and have been shown to be biocompatible with different cells [21, 43]. The cytotoxicity of ZnONWs@AgNPs was evaluated with human embryonic kidney cell line 293 and rat embryonic smooth muscle cell line A7R5 cells by 3-(4,5-dimethylthiazol-2-yl)-2,5-diphenyl tetrazolium bromide (MTT) assays. ZnONWs@AgNPs were collected from the Ag/ZnO/textile composites and incubated with 293 cells and A7R5 cells. After 24, 48 and 72 h of incubation, it is found that the ZnONW@AgNP nanostructures have little influence on cells at low concentrations (0.01 μg ml^{-1}), and only led to a mild decrease of cell viability (~25%) at high concentration (10 μg ml^{-1}), as shown in figure 3 and figure S3 (available at stacks.iop.org/Nano/25/145702/mmedia) respectively, which suggested that the ZnONW@AgNP nanocomposites have reasonably good biocompatibility to human and mammalian cells. Considering the good cellular biocompatibility of ZnO NWs [21], the combined ZnONW@AgNP structure may reduce the dispersion of AgNPs and abate cytotoxicity.

To investigate the antimicrobial activity of the Ag/ZnO/textile composites, both gram-negative bacteria *E. coli* HB101 and gram-positive bacteria *Staphylococcus aureus* (*S.a.*, ATCC 25923) were incubated with the composites. The zone of inhibition in the modified Kirby–Bauer test and microbial viability of bacteria in the colony-forming unit (CFU) test were measured to evaluate the antimicrobial activity of the composites. The modified Kirby–Bauer zone of inhibition test method is used to evaluate the antibacterial activity of the composites qualitatively. Parallel experiments were conducted with pure textile, ZnO/textile, Ag20/ZnO/textile and the well documented commercial antimicrobial nanocrystalline silver dressing ACTICOAT^{TM} (Smith and Nephew), respectively. ACTICOAT^{TM} is a well known commercial antimicrobial

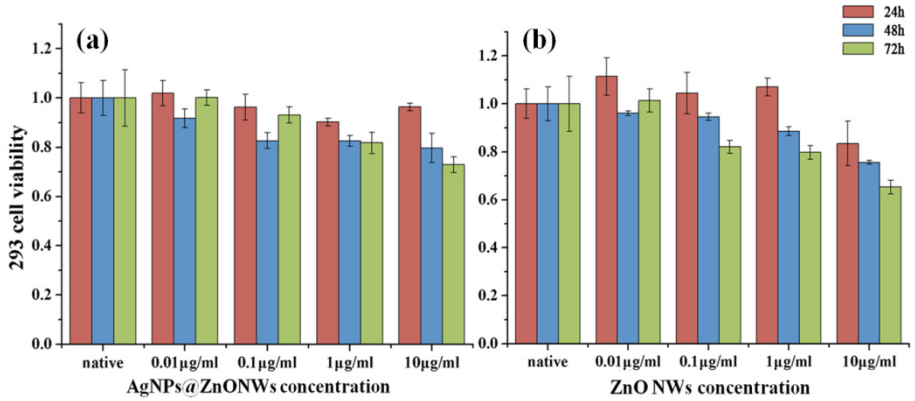

Figure 3. MTT test for investigating the biocompatibility of ZnO NWs and ZnONWs@AgNPs in human embryonic kidney cell line 293. (a) The viability of 293 cells incubated with ZnONW@AgNP nanostructures for 24, 48 and 72 h. (b) The viability of 293 cells by incubated with ZnO NWs for 24, 48 and 72 h. Both ZnONWs@AgNPs and ZnO NWs have little influence on cellular viability in different concentrations from 0.01 to 10 μg ml^{-1}.

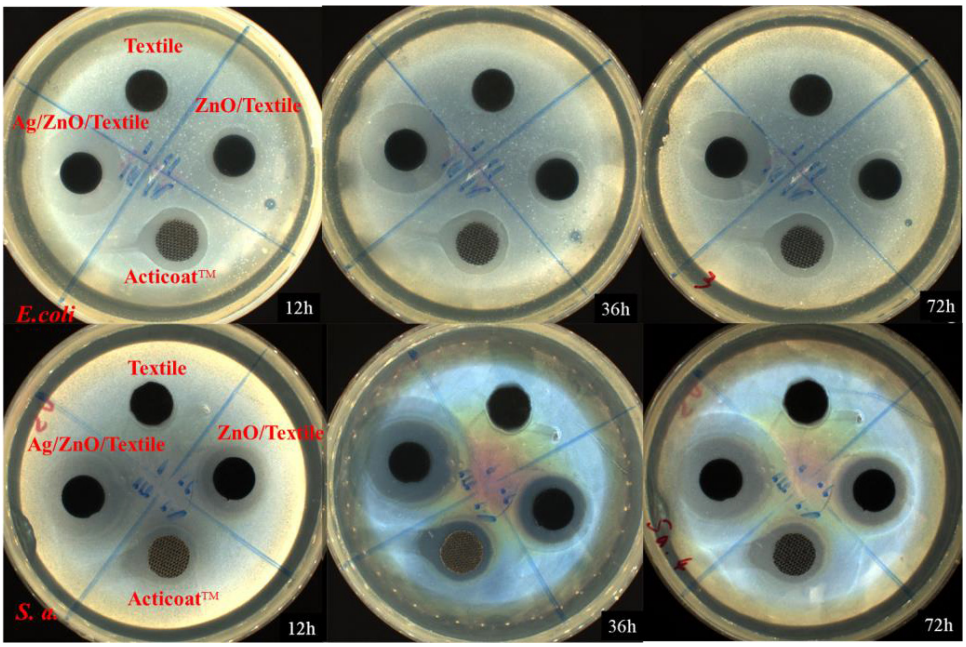

Figure 4. A modified Kirby–Bauer method is used to evaluate the zone of inhibition of four different materials. Pure textile, ZnO/textile, the commercial ACTICOAT^{TM} and Ag/ZnO/textile (Ag20) are cut into disks ($\varphi = 11$ mm) and placed on a lawn of *E. coli*/*S.a.* on an agar medium plate. By incubating at 37 °C for 72 h, the clear ring of the inhibition zone can be easily observed and measured for investigating the diffusion of antibacterial activity. For both gram-negative and gram-positive bacteria, the inhibition zone of Ag/ZnO/textile is significantly larger than those of the other three materials.

dressing with nanocrystalline silver, applied in clinical burned skin coverings [44, 45].

Each textile material was cut into a disk ($\varphi = 11$ mm) and placed in a quadrant of an agar plate with *E. coli*/*S.a.*, sharing with other three disks of different loading materials (figure 4). The antibacterial activity of the samples can be evaluated by the smallest clear ring of the zone of inhibition. The plate was incubated at 37 °C for 72 h and the diameters of the zones of inhibition were measured every 12 h. In the first 12 h, clear zone of inhibition regions appeared around the Ag20, ZnO/textile and ACTICOAT^{TM} samples on the agar medium, suggesting that bacteria surrounding these materials were inhibited or perished. As expected, the pure textile, which has no antibacterial activity, exhibits no zone of inhibition on the agar medium. These results suggest that the antibacterial activity of ZnO/textile came from the ZnO and the antibacterial activity of Ag20 came from both ZnO and the Ag nanoparticles decorated on the ZnO NWs.

We also finished the statistical study of the modified Kirby–Bauer tests in the four investigated materials in the culture of *E. coli* and *S.a.* (figure 5) The columns in figure 5(a) show the diameter of the zone of inhibition of pure textile, ZnO/textile, ACTICOAT^{TM} and Ag20 composites. The zone of inhibition in gram-negative bacteria is about 11 mm, 15 mm,

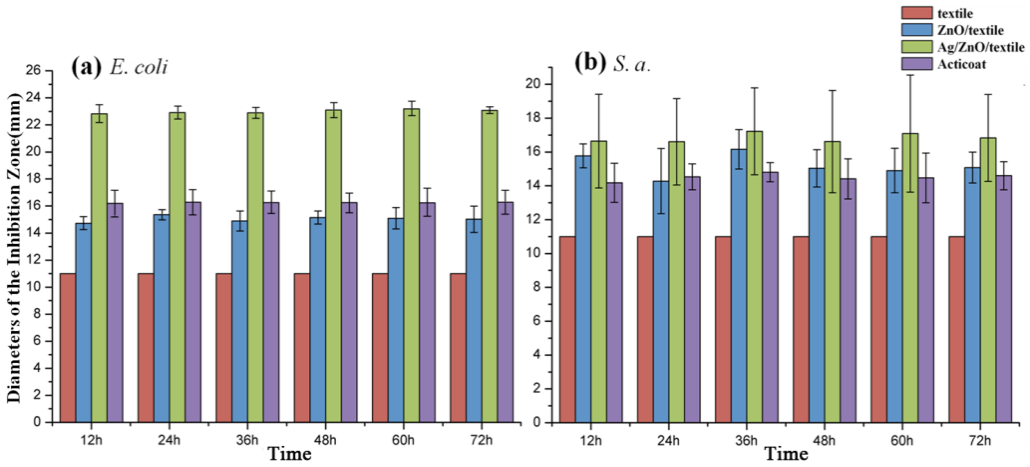

Figure 5. The columns exhibit the diameter of the inhibition zone of four different materials in gram-negative *E. coli* (a) and gram-positive *S.a.* (b) bacteria. (a) The inhibition zone of *E. coli*. Ag/ZnO/textile (Ag20) hybrid has the largest inhibition zone, about 23 mm in diameter. (b) The inhibition zone of *S.a.* The diameter of the inhibition zone shows a similar relationship to that of *E. coli*. Pure textile has no inhibition zone. The diameter of the inhibition zone has almost no change from 12 to 72 h, suggesting long-term antibacterial activity of the Ag/ZnO/textile hybrid.

16 mm and 23 mm, respectively. As known in advance, the zone of inhibition of pure textile is the diameter of the disk. The columns in figure 5(b) show the results in gram-positive bacteria. The zone of inhibition of Ag20 composites is also larger than those of ACTICOAT^{TM}, ZnO/textile and pure textile.

Remarkably, the Ag20 sample shows very steady and long-term antibacterial activity, even comparing with the commercial antimicrobial dressing ACTICOAT^{TM}. From 12 to 72 h, the diameters of zone of inhibition remain unchanged as time elapses (figure 5), suggesting the Ag20 can preserve a high antibacterial activity in both gram-negative *E. coli* and gram-positive *S.a.* bacteria. Besides, with the modified Kirby–Bauer test continued for 72 h, the Ag20 presents a long-term inhibition of proliferation in both gram-negative and gram-positive bacteria.

A parallel study was conducted between Ag20, Ag100 and ACTICOAT^{TM} by a modified Kirby–Bauer method. ACTICOAT^{TM} dressing contains at least eight times more silver atoms than Ag/ZnO/textile composites (table S1 available at stacks.iop.org/Nano/25/145702/mmedia), and the diameters of silver particles in ACTICOAT^{TM} are in the range of hundreds of nanometers. In the modified Kirby–Bauer test, Ag20 and Ag100 show potent antibacterial activity against both gram-negative *E. coli* and gram-positive *S.a.* bacteria. The diameters of the zone of inhibition for Ag20 and Ag100 are very close to each other in both gram-negative and gram-positive bacteria (figure S2 available at stacks.iop.org/Nano/25/145702/mmedia), while both of them are larger than that of ACTICOAT^{TM}. Our observations are consistent with previous studies showing that gram-positive bacteria are more resistant to AgNPs since their membranes are thicker and more stable than those of gram-negative bacteria [37].

This result indicates that the antibacterial activity of Ag/ZnO/textile in the Kirby–Bauer test is higher than that of ACTICOAT^{TM}, which is probably due to the high specific surface areas and the enhanced ion release of Ag NPs. The ZnO NWs also play an important role here due to the synergistic effect. Besides, Xiu *et al* infer that Ag NP morphological properties primarily influence release of Ag^+, and Ag^+ is the definitive molecular toxicant to bacteria [46]. Their theory gives us a clue to understand our result: Ag20 and Ag100 have much lower quantities of silver than ACTICOAT^{TM} but they have high dispersity and high specific surface, which are advantages for Ag^+ release. The Ag20 and Ag100 release more Ag^+ ions than ACTICOAT^{TM} within the same period of time, thus they exhibit higher antibacterial activity.

The CFU test estimates the number of viable germs, which are able to form visible colonies on agar medium, after treatment with antibacterial materials. This experiment evaluates the antibacterial activity of our nanocomposites by direct contact. The Ag100 sample is chosen as a reference to compare its antibacterial activity with one of the other three materials: Ag20, ZnO/textile and ACTICOAT^{TM}. The solutions of gram-positive *S.a.* bacteria were shaken with antibacterial materials for some hours to ensure full contact between antibacterial materials and bacteria. The solution was then diluted, spread uniformly on an agar plate and incubated at 37 °C. The number of bacterial colonies on the agar plates is counted by using a colony-counter 24 h later and we calculate the number of CFUs with the following formula:

$$\text{CFU counts} = \frac{\text{colony counts}}{\text{dilution ratio} \times \text{amount of sample}}. \quad (4)$$

The CFU results are shown in figure 6. It shows that ZnO/textile deactivates 58.1, 67.4 and 99.6% of bacteria after shaking with samples for 1, 2 and 5 h, respectively. Remarkably, Ag100 deactivates approximately 99.5% of the bacteria in the first hour (table S2 available at stacks.iop.org/Nano/25/145702/mmedia), and this value is increased to more than 99.99% after shaking for 2 h. The antibacterial activity of Ag100 is two to four orders higher than ZnO/textile. This result indicates that the *in situ* synthesized Ag NPs enhance the antibacterial activity of ZnO/textile significantly.

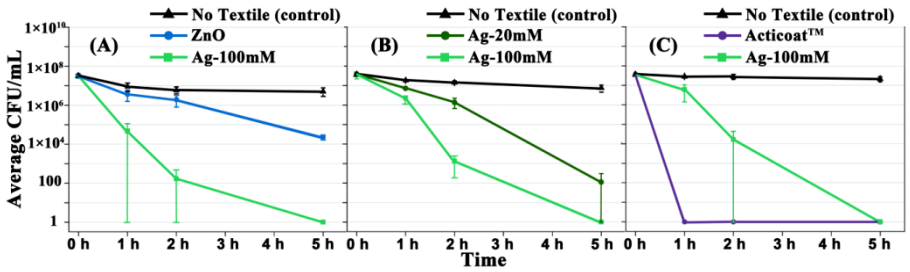

Figure 6. A parallel study between ZnO/textile, Ag20, Ag100 and ACTICOAT™ in a CFU test. The three samples treat bacterial medium for 1, 2 and 5 h. (a) A comparison of CFU between ZnO/textile and Ag100. The lower line indicates the Ag100 has a higher antibacterial activity, about two to four orders of magnitude higher than ZnO. (b) A comparison of CFU between Ag20 and Ag100. The CFU curve of Ag100 is lower than that of Ag20. The antibacterial activity of Ag100 is one to three orders of magnitude higher than that of Ag20. (c) A comparison of CFU between Ag100 and ACTICOAT™. After 1 and 2 h treatment, ACTICOAT™ represents a higher antibacterial activity than Ag100. After 5 h treatment, the CFU results of ACTICOAT™ and Ag100 are the same.

The result of the CFU test between Ag20 and Ag100 shows that fewer bacteria; colonies are counted after treatment with Ag100 (figure 6(b)). In the first hour, Ag100 deactivates 87.8% of bacteria, and Ag20 61.5%. After 5 h, Ag100 and Ag20 both deactivate nearly 100% of bacteria in our experiment, respectively. In figure 6(b), Ag100 shows a more efficient antibacterial activity, about one to three orders of magnitude higher than that of Ag20. This result probably originates from the difference of Zn and Ag atomic ratio between the two materials, which is surveyed through EDX and is shown in table S1 (available at stacks.iop.org/Nano/25/145702/mmedia). The Ag100 sample contains 10.5 wt% of silver atoms and the Ag20 sample 6.1 wt%. This indicates that the antibacterial activity is positively correlated with the number of Ag NPs on ZnO NWs. More Ag NPs can increase the opportunity of contact between Ag and bacteria, and deactivate more bacteria.

The CFU test shows that the commercial ACTICOAT™ manifests more efficient antibacterial activity than Ag100, with over 99.99% of the bacteria killed within the first hour (figure 6(c)). However, from 2 to 5 h, the CFU counts of Ag100 decrease remarkably and attain the same level as ACTICOAT™. After 5 h, the Ag100 and ACTICOAT™ deactivate nearly 100% of bacteria (table S2 available at stacks.iop.org/Nano/25/145702/mmedia). The silver atoms in ACTICOAT™ are at 86.5 wt%, significantly greater than in Ag100 (10.5 wt%). The massive Ag NPs in ACTICOAT™ play an important role in its antibacterial activity by direct contact. However, the difference of antibacterial activity between Ag100 and ACTICOAT™ is tiny, especially after long contact periods. It is reasonable to believe that the antibacterial activity of our nanocomposites can match or even exceed the effect of ACTICOAT™ if the quantity of silver in our nanocomposites is increased.

As we pointed out, the aggregation of Ag NPs, the long-term antibacterial activity and the dangerous exposures of silver in the environment are three key obstacles for practical applications of silver nanostructures. Here, we discuss the obvious advantage of Ag/ZnO/textile nanocomposites to solve these three problems.

The long-term antibacterial activity was evaluated by a modified Kirby–Bauer test. Ag/ZnO/textile nanocomposites exhibit potent antibacterial activity and inhibit both gram-negative and gram-positive bacterial proliferation for at least 72 h, demonstrating long-term antibacterial activity of the composites.

Furthermore, we found that the Ag/ZnO/textile nanocomposites can be reused many times to inhibit bacteria. After the first 72 h modified Kirby–Bauer test, all disks were taken up from agar plates and placed directly on new agar plates incubated with bacteria, without any treatment. The modified Kirby–Bauer test was carried out several times, with an incubation time of 72 h in each test.

The results are shown in tables S3 and S4 (available at stacks.iop.org/Nano/25/145702/mmedia). The zone of inhibition induced by Ag/ZnO/textile nanocomposites can be clearly identified, from the first to the fourth modified Kirby–Bauer test. It is remarkable that the nanocomposites preserve a long-term antibacterial activity after multiple times of use. SEM images are taken of the reused nanocomposites. The ZnONW@AgNP nanostructures finely remain on the textile after being taken up from agar (figure S5 available at stacks.iop.org/Nano/25/145702/mmedia). Simultaneously, ZnO NWs sustain Ag NPs from self-aggregation and bind with these nanoparticles. The ZnONW@AgNP structure plays a key role for long-term antibacterial activity and makes this textile recoverable and reusable. The antibacterial activity of ACTICOAT™ with respect to *E. coli* decreases significantly after the third test. Silver particles on ACTICOAT™ are easily flaked off and adhered on the agar medium, which is easily seen by the naked eye. This may be the reason for its invalidation.

Simultaneously, the Ag NPs are synthesized by the 'dip-in and light-irradiation' green chemical method without toxic chemical agents. From the TEM image of ZnONWs@AgNPs in figure 2(b), we can find that the Ag NPs were completely attached to the ZnO NWs without aggregation, and this ZnONW@AgNP nanostructure is finely preserved after antibacterial test (figure S5 available at stacks.iop.org/Nano/25/145702/mmedia) to insure the Ag NPs separate. Another benefit of the ZnONW@AgNP nanostructures on textile is easy to take off and thus reduce the harmful silver exposures, which is very important while considering the environmental impact. Once the antibacterial process is accomplished, silver nanoparticles can be recycled very conveniently.

3. Conclusion

In summary, we demonstrate a new approach of a long-term and recoverable antimicrobial nanostructure/textile hybrid without increasing the antimicrobial resistance of bacteria. Using *in situ* synthesized Ag NPs anchoring on ZnO NWs grown on textiles by a 'dip-in and light-irradiation' green chemical method, we obtained ZnONW@AgNP nanocomposites with small-sized Ag NPs with relative uniform diameters. The ZnONWs@AgNPs address four major superiorities simultaneously. ZnO NWs can prevent the aggregation of Ag NPs, which ensures the long-term antimicrobial activity of the nanocomposites. Meanwhile, green synthesis of Ag NPs without external toxic and corrosive reducing agents, organic solvents and stabilizer is another environmentally benign process to avoid potential biological risk and to enable practical applications. The nanocomposites are reusable and can be easily reclaimed by simply taking up textiles from applied surface for reducing silver exposure in environment. Finally, the biocompatible ZnO NWs are antimicrobial material, which can provide additional antimicrobial ability to Ag NPs by a synergistic effect. Thus, the use of ZnO NWs will not cause extra biological risk, while promoting the antimicrobial effect. The hybrid shows potent, steady and long-term antibacterial activity for wide medical and environmental applications. This new Ag/ZnO/textile antimicrobial composite can be used for wound dressings and medical textiles for topical and prophylactic antibacterial treatments, point-of-use water treatment to improve the cleanliness of water and antimicrobial air filters to prevent bioaerosols accumulating in ventilation, heating and air-conditioning systems.

Acknowledgments

The work was supported by the NSFC (No 31200702, 11120101001,10925208, 50772024, 11202018), Beijing Municipal Natural Science Foundation (No 713212), NCET-12-0027, Beijing Nova Program (Z121103002512019), the RFDP (20111102120038), the Knowledge Innovation Program of the Chinese Academy of Sciences (KJCX2-YWM13), and the National Basic Research Program of China (2009CB930702).

References

[1] William K 2000 Antibiotics, invention and innovation *Res. Policy* **29** 679–710
[2] Blaser M 2011 Antibiotic overuse: stop the killing of beneficial bacteria *Nature* **476** 393–4
[3] Schmidt M A, Smith L H and Sehnert K W 1993 *Beyond Antibiotics: 50 (or so) Ways to Boost Immunity and Avoid Antibiotics* 2nd edn (Berkeley, CA: North Atlantic Books)
[4] Walsh T R, Weeks J, Livermore D M and Toleman M A 2011 Dissemination of NDM-1 positive bacteria in the New Delhi environment and its implications for human health: an environmental point prevalence study *Lancet Infect. Dis.* **11** 355–62
[5] Around the World 2011 Superbug gene found in tap water *Science* **332** 288–9
[6] www.who.int/world-health-day/2011/en/
[7] Sondi I and Salopek-Sondi B 2004 Silver nanoparticles as antimicrobial agent: a case study on E. coli as a model for Gram-negative bacteria *J. Colloid Interface Sci.* **275** 177–82
[8] Marambio-Jones C and Hoek E M 2010 A review of the antibacterial effects of silver nanomaterials and potential implications for human health and the environment *J. Nanopart. Res.* **12** 1531–51
[9] Morones J R, Elechiguerra J L, Camacho A, Holt K, Kouri J B, Ramírez J T and Yacaman M J 2005 The bactericidal effect of silver nanoparticles *Nanotechnology* **16** 2346–53
[10] Gogoi S K, Gopinath P, Paul A, Ramesh A, Ghosh S S and Chattopadhyay A 2006 Green fluorescent protein-expressing *Escherichia coli* as a model system for investigating the antimicrobial activities of silver nanoparticles *Langmuir* **22** 9322–8
[11] Rai M, Yadav A and Gade A 2009 Silver nanoparticles as a new generation of antimicrobials *Biotechnol. Adv.* **27** 76–83
[12] Feng Q L, Wu J, Chen G Q, Cui F Z, Kim T N and Kim J O 2000 A mechanistic study of the antibacterial effect of silver ions on *Escherichia coli* and *Staphylococcus aureus* *J. Biomed. Mater. Res.* **52** 662–8
[13] Liau S Y, Read D C, Pugh W J, Furr J R and Russell A D 1997 Interaction of silver nitrate with readily identifiable groups: relationship to the antibacterial action of silver ions *Lett. Appl. Microbiol.* **25** 279–83
[14] Matsumura Y, Yoshikata K, Kunisaki S-I and Tsuchido T 2003 Mode of bactericidal action of silver zeolite and its comparison with that of silver nitrate *Appl. Environ. Microbiol.* **69** 4278–81
[15] Wong K Y and Liu X 2010 Silver nanoparticles—the real 'silver bullet' in clinical medicine? *Med. Chem. Commun.* **1** 125–31
[16] Liu L, Liu J, Wang Y, Yan X and Sun D D 2011 Facile synthesis of monodispersed silver nanoparticles on graphene oxide sheets with enhanced antibacterial activity *New J. Chem.* **35** 1418–23
[17] Lv M, Su S, He Y, Huang Q, Hu W, Li D, Fan C and Lee S-T 2010 Long-term antimicrobial effect of silicon nanowires decorated with silver nanoparticles *Adv. Mater.* **22** 5463–7
[18] Dankovich T A and Gray D G 2011 Bactericidal paper impregnated with silver nanoparticles for point-of-use water treatment *Environ. Sci. Technol.* **45** 1992–8
[19] Vaidyanathan R, Kalishwaralal K, Gopalram S and Gurunathan S 2009 Retraction: Nanosilver–the burgeoning therapeutic molecule and its green synthesis *Biotechnol. Adv.* **27** 924–37
[20] Sharma V K, Yngard R A and Lin Y 2009 Silver nanoparticles: green synthesis and their antimicrobial activities *Adv. Colloid Interface Sci.* **145** 83–96
[21] Li Z, Yang R, Yu M, Bai F, Li C and Wang Z L 2008 Cellular level biocompatibility and biosafety of ZnO nanowires *J. Phys. Chem.* C **112** 20114–7
[22] Pan Z W, Dai Z R and Wang Z L 2001 Nanobelts of semiconducting oxides *Science* **291** 1947–9
[23] Tang H Y, Ding Y, Jiang P, Zhou H Q, Guo C F, Sun L F, Yu A F and Wang Z L 2011 High-index facets bound ripple-like ZnO nanobelts grown by chemical vapor deposition *Cryst. Eng. Comm.* **13** 5052–4
[24] Li H Y, Quan B G, Tang H Y, Guo C F, Jiang P, Yu A F, Xie S S and Wang Z L 2011 ZnO nanowire arrays with and without cavity tops *Mater. Chem. Phys.* **129** 905–9

[25] Xu S and Wang Z L 2011 One-dimensional ZnO nanostructures: solution growth and functional properties *Nano Res.* **4** 1013–98
[26] Li Z, Zhu G, Yang R, Wang A C and Wang Z L 2010 Muscle-driven *in vivo* nanogenerator *Adv. Mater.* **22** 2534–7
[27] Yeh P H, Li Z and Wang Z L 2009 Schottky-gated probe-free ZnO nanowire biosensor *Adv. Mater.* **21** 4975–8
[28] Nie L, Gao L, Feng P, Zhang J, Fu X, Liu Y, Yan X and Wang T 2006 Three-dimensional functionalized tetrapod-like ZnO nanostructures for plasmid DNA delivery *Small* **2** 621–5
[29] Zhang P and Liu W 2010 ZnO QD@PMAA-co-PDMAEMA nonviral vector for plasmid DNA delivery and bioimaging *Biomaterials* **31** 3087–94
[30] Hong H, Shi J, Yang Y, Zhang Y, Engle J W, Nickles R J, Wang X and Cai W 2011 Cancer-targeted optical imaging with fluorescent zinc oxide nanowires *Nano Lett.* **11** 3744–50
[31] Wang Z L 2008 Self-powered nanotech *Sci. Am.* **298** 82–7
[32] Lieber C M and Wang Z L 2007 Functional nanowires *MRS Bull.* **32** 99–108
[33] Wang Z L 2010 Piezopotential gated nanowire devices: piezotronics and piezo-phototronics *Nano Today* **5** 540–52
[34] Lew Y V L and Willatzen M 2011 Electromechanical phenomena in semiconductor nanostructures *J. Appl. Phys.* **109** 031101
[35] Yang Y, Qi J, Liao Q, Li H, Wang Y, Tang L and Zhang Y 2009 High-performance piezoelectric gate diode of a single polar-surface dominated ZnO nanobelt *Nanotechnology* **20** 125201
[36] Koga H, Kitaoka T and Wariishi H 2009 *In situ* synthesis of silver nanoparticles on zinc oxide whiskers incorporated in a paper matrix for antibacterial applications *J. Mater. Chem.* **19** 2135–40
[37] Lu W, Liu G, Gao S, Xing S and Wang J 2008 Tyrosine-assisted preparation of Ag/ZnO nanocomposites with enhanced photocatalytic performance and synergistic antibacterial activities *Nanotechnology* **19** 445711
[38] Karunakaran C, Rajeswari V and Gomathisankar P 2011 Enhanced photocatalytic and antibacterial activities of sol–gel synthesized ZnO and Ag–ZnO *Mater. Sci. Semicond. Process.* **14** 133–8
[39] Karunakaran C, Rajeswari V and Gomathisankar P 2011 Combustion synthesis of ZnO and Ag-doped ZnO and their bactericidal and photocatalytic activities *Superlatt. Microstruct.* **50** 234–41
[40] Tang H Y, Liu T J and Jiang P 2013 ZnO nanowires grown on carbon cloth for flexible cold cathode *J. Nanosci. Nanotechnol.* **13** 1385–8
[41] Alammar T and Mudring A V 2009 Facile preparation of Ag/ZnO nanoparticles via photoreduction *J. Mater. Sci.* **44** 3218–22
[42] Shvalagin V V, Stroyuk A L and Kuchmii S Y 2007 Photochemical synthesis of ZnO/Ag nanocomposites *J. Nanopart. Res.* **9** 427–40
[43] Podsiadlo P, Paternel S, Rouillard J M, Zhang Z, Lee J, Lee J W, Gulari E and Kotov N A 2005 Layer-by-layer assembly of nacre-like nanostructured composites with antimicrobial properties *Langmuir* **21** 11915–21
[44] www.smith-nephew.com/uk/products/wound_management/product-search/acticoat/
[45] Gravante G, Caruso R, Sorge R, Nicoli F, Gentile P and Cervelli V 2009 Nanocrystalline silver: a systematic review of randomized trials conducted on burned patients and an evidence-based assessment of potential advantages over older silver formulations *Ann. Plast. Surg.* **63** 201–5
[46] Xiu Z, Zhang Q, Puppala H L, Colvin V L and Alvarez P J J 2012 Negligible particle-specific antibacterial activity of silver nanoparticles *Nano Lett.* **12** 4271–5